ARCHIVES OF ELECTRICAL ENGINEERING VOL. 67(2), pp. 345–359 (2018)

DOI 10.24425/119645

Directional change and windup phenomena in LQR-controlled systems with actuator failure

DARIUSZ HORLA

Poznan University of Technology, Faculty of Electrical Engineering
Institute of Control, Robotics and Information Engineering
ul. Piotrowo 3a, 60-965 Poznań, Poland
e-mail: dariusz.horla@put.poznan.pl

(Received: 17.08.2017, revised: 10.10.2017)

Abstract: The paper presents a phenomenon of directional change in the case of a LQR controller applied to multivariable plants with amplitude and rate constraints imposed on the control vector, as well as the impact of the latter on control performance, with the indirect observation of the windup phenomenon effect via frequency of consecutive resaturations. The interplay of directional change of the computed control vector with control performance has been thoroughly investigated, and it is a result of the presence of constraints imposed on the applied control vector for different ratios of the number of control inputs to plant outputs. The impact of the directional change phenomenon on the control performance (and also on the windup phenomenon) has been defined, stating that performance deterioration is not tightly coupled with preservation of direction of the computed control vector. This conjecture has been supported by numerous simulation results for different types of plants with different LQR controller parameters.

Key words: directional change, windup phenomenon, actuator failure

1. Introduction

The robust control problem is widely discussed in the current references, with a group of papers relating to measuring performance in the sense of a quadratic cost function when uncertainty is taken into account, see, e.g. the references for continuous-time systems [8] or [9]. For discrete-time closed-loop systems the reliable control, ensuring the bound of the cost, has been discussed in [11].

Reliability means that whenever actuator failure occurs, the controller must ensure the proper level of performance, to maintain such properties of the closed-loop system as stability or moderate tracking performance. In the current paper, the approach presented in [12] is used to analyze the interplay between directional change in controls and an actuator failure case. The actuator failure itself is used to mimic the possible situation, when a computed control signal/vector is modified by a nonlinear block, here: saturation that changes the proportions between components of the calculated control vector, resulting in the directional change phenomenon.

The real-world systems are subject to cut-off (saturation) actuator constraints limiting controller outputs, which have a negative impact on the control performance, and actuator saturation, consequently, causes lack of consistency between computed and constrained control inputs, referred as the windup phenomenon. The stability analysis results of saturated control systems may be found in, e.g. [5, 10].

The state-feedback control law is proposed here to ensure reliability of the system with failures modeled by the scaling factors, which are used to present the uncertainty, and are depicted as conic areas in the space of control signals on the static characteristics of the considered nonlinearity, here: a saturation function.

It is of practical importance to identify the interplay between directional change and performance of the control system. This aspect of the directional change is often not present in the literature referring to the windup phenomenon, and is virtually not addressed in papers concerning multivariable control systems. Whereas, in the case of multivariable systems possible cross-coupling and the unequal number of plant inputs and outputs are important factors. The direction of the calculated control vector might reflect principal input direction [6, 7]/maximal directional gain [1], but it can also be connected to possibility to decouple inputs from outputs in dynamic states. By changing this information, the performance of the control system might seriously deteriorate.

As an example, one can take the nonlinear chemical Van de Vusse reaction presented in [14], where it is required to control concentration of the intermediate and final products by dilution rate inputs, maintaining them in proportions, and in accordance to possible limits, to prevent the system from changing its properties. Another example, could be a control regime of an UAV [2], in which in order to keep the drone in a horizontal position when ascending or descending, thrust forces of the motors must be kept in proportion, by ensuring equal rotational speeds of the rotors. Possible saturations of control signals in dynamical states, require the control system to preserve the direction of the control vector.

2. Plant and actuator failure models

The following multivariable model is taken into consideration:

$$\boldsymbol{x}_{t+1} = \boldsymbol{A}\boldsymbol{x}_t + \boldsymbol{B}\boldsymbol{u}_{t-d}\,, \tag{1}$$

$$\boldsymbol{y}_t = \boldsymbol{C}\boldsymbol{x}_t\,, \tag{2}$$

where the left-coprime polynomial matrices:

$$\boldsymbol{A}(q^{-1}) = \boldsymbol{I} + \boldsymbol{A}_1 q^{-1} + \cdots + \boldsymbol{A}_{n\boldsymbol{A}} q^{-n\boldsymbol{A}}, \tag{3}$$

$$\boldsymbol{B}(q^{-1}) = \boldsymbol{B}_0 + \boldsymbol{B}_1 q^{-1} + \cdots + \boldsymbol{B}_{n\boldsymbol{B}} q^{-n\boldsymbol{B}} \tag{4}$$

have known sizes ($i = 1, \ldots, n\boldsymbol{A}$, $j = 0, \ldots, n\boldsymbol{B}$):

$$\boldsymbol{A}_i \in \mathrm{R}^{p\times p}, \tag{5}$$

$$\boldsymbol{B}_j \in \mathsf{R}^{p\times m} \tag{6}$$

and degrees $n\boldsymbol{A}$, $n\boldsymbol{B}$. The output vector $\boldsymbol{y} \in \mathsf{R}^p$, the constrained control vector $\boldsymbol{u} \in \mathsf{R}^m$, the computed control vector $\boldsymbol{v} \in \mathsf{R}^m$, and the state vector $\boldsymbol{x} \in \mathsf{R}^n$, which is exactly known.

The control performance index is defined as in standard LQR control laws:

$$J = \sum_{t=0}^{\infty} \left(\boldsymbol{x}_t^T \boldsymbol{Q}\boldsymbol{x}_t + \boldsymbol{u}_t^T \boldsymbol{R}\boldsymbol{u}_t\right), \tag{7}$$

with weighing matrices $\boldsymbol{Q} \geq 0$, $\boldsymbol{R} \geq 0$. The actuator failure model can be defined as in [15]:

$$u_{t,i}^k = (1-\rho_{t,i}^k)\mathrm{sat}(v_{t,i};\alpha_i) \qquad (i = 1,\ 2,\ \ldots,\ m, \quad k = 1,\ 2,\ \ldots,\ g), \tag{8}$$

where $\rho_{t,i}^k$ is an unknown constant from some range, index k denotes the k-th failure model, and g is the total number of failure models. The expression $u_{t,i}^k$ refers to the i-th component of the constrained control vector, assuming that an actuator failure takes place (in the other case, $u_{t,i}^k = v_{t,i}$). For any actuator failure model, including the situation for constraints imposed on the control vector, the constant $\rho_{t,i}^k$ lies in $\rho_{-,t,i}^k \leq \rho_{t,i}^k \leq \rho_{+,t,i}^k$, and the function sat defines the method od applying constraints (e.g. cut-off constraint).

The control vector might be modified by various functions, such as cut-off constraints, nonlinear static characteristics, or by a direction-preserving (DP) saturation algorithm. The difference between non-DP and DP cut-off functions is discussed in the paper.

If $\rho_{-,t,i}^k = \rho_{+,t,i}^k = 0$ holds, it means that failure (8) has not taken place, and $\rho_{-,t,i}^k = \rho_{+,t,i}^k = 1$ corresponds to the outage case in the k-th failure model. The failure according to the k-th model means that $0 < \rho_{-,t,i}^k \leq \rho_{+,t,i}^k < 1$ is satisfied.

For a single model case of the failure, (8) can be transformed [12, 13, 4] to

$$u_{t,i}^F = \rho_i v_{t,i} \quad (i = 1,\ 2,\ \ldots,\ m), \tag{9}$$

where

$$0 \leq \rho_{-,i} \leq \rho_i \leq \rho_{+,i} \quad (i = 1,\ 2,\ \ldots,\ m) \tag{10}$$

with $\rho_{-,i} \leq 1$ and $\rho_{+,i} \geq 1$.

The following notation is henceforth adopted from [13, 4]:

$$\boldsymbol{u}_t^T = \left[u_{t,1}^F,\ u_{t,2}^F,\ \ldots,\ u_{t,m}^F\right]^T, \tag{11}$$

$$\boldsymbol{\rho}_+ = \mathrm{diag}\left\{\rho_{+,1}, \rho_{+,2}, \ldots, \rho_{+,m}\right\}, \tag{12}$$

$$\boldsymbol{\rho}_- = \mathrm{diag}\left\{\rho_{-,1}, \rho_{-,2}, \ldots, \rho_{-,m}\right\}, \tag{13}$$

$$\boldsymbol{\rho} = \mathrm{diag}\left\{\rho_1, \rho_2, \ldots, \rho_m\right\}. \tag{14}$$

3. Directional change phenomenon

The directional change might be observed in majority of cases which is presented in Fig. 1a, in the case of cut-off saturation. Lack of the directinonal change depends on the way the saturation is performed (dashed lines) for constant direction requirement, Fig. 1b.

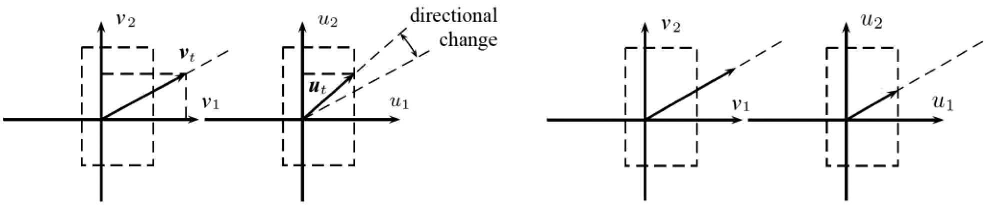

Fig. 1. (a) Direction-changing; (b) direction-preserving saturation (left – control vector before amplitude saturation, right – after saturation)

4. Control law

The control law of the form:

$$\boldsymbol{v}_t = \boldsymbol{F}\boldsymbol{x}_t\,, \tag{15}$$

where $\boldsymbol{x}_t$ is the state vector of the plant models (1), (2), it is reliable (value of the performance index (7) is not exceeded), when it is related to the matrix $\boldsymbol{P}$, the systems (1), (2), and if $\boldsymbol{P}$ satisfies the inequality [4, 13]

$$(\boldsymbol{A}+\boldsymbol{B}\rho\rho)^T\boldsymbol{P}(\boldsymbol{A}+\boldsymbol{B}\rho\rho)-\boldsymbol{P}+\boldsymbol{F}^T\rho\boldsymbol{R}\rho\boldsymbol{F}+\boldsymbol{Q}\leq 0\,. \tag{16}$$

The closed loop system:

$$\boldsymbol{x}_{t+1} = (\boldsymbol{A}+\boldsymbol{B}\rho\rho)\boldsymbol{x}_t \tag{17}$$

is then stable, and it holds that

$$J=\sum_{t=0}^{\infty}\boldsymbol{x}_t^T\left(\boldsymbol{Q}+\boldsymbol{F}^T\rho\boldsymbol{R}\rho\boldsymbol{F}\right)\boldsymbol{x}_t\leq \boldsymbol{x}_0^T\boldsymbol{P}\boldsymbol{x}_0\,. \tag{18}$$

When robustness issues are not taken into accoung, the optimal $\boldsymbol{F}$ in (15) is derived as the solution of the set of equations [4]:

$$\boldsymbol{F}=-\left(\boldsymbol{B}^T\boldsymbol{P}\boldsymbol{B}+\boldsymbol{R}\right)^{-1}\boldsymbol{B}^T\boldsymbol{P}\boldsymbol{A}\,, \tag{19}$$

$$\boldsymbol{P}=\boldsymbol{Q}+\boldsymbol{A}^T\boldsymbol{P}\boldsymbol{A}-\boldsymbol{A}^T\boldsymbol{P}\boldsymbol{B}\left(\boldsymbol{B}^T\boldsymbol{P}\boldsymbol{B}+\boldsymbol{R}\right)^{-1}\boldsymbol{B}^T\boldsymbol{P}\boldsymbol{A}\,, \tag{20}$$

the optimal value $J_{\boldsymbol{F}}$ of the performance index (7), based on obtaining $\boldsymbol{F}$ according to (19) and (20) being at the same time the upper boundary of (18), is:

$$J_{\boldsymbol{F}} = \boldsymbol{x}_0^T\boldsymbol{P}\boldsymbol{x}_0\,. \tag{21}$$

5. Optimal state-feedback matrix in the case of actuator failure

This section of the paper has been taken in extenso from [3], since it cannot be omitted here, to ensure the paper is coherent. The below algorithm [4, 13] enabling derivation of the optimal state-feedback matrix $\boldsymbol{F}$ to increase the robustness of the system against actuator failure can be adopted for both DP and non-DP functions:

1. Solve (20) with respect to $\boldsymbol{P}$ (mark the result as $\boldsymbol{P}^*$), and choose an arbitrary diagonal matrix $\boldsymbol{R}_0$, satisfying

$$\boldsymbol{R}_0 \leq \left(\boldsymbol{B}^T\boldsymbol{P}^*\boldsymbol{B}+\boldsymbol{R}\right)^{-1}. \tag{22}$$

2. Solve

$$\boldsymbol{P} = \boldsymbol{Q}+\boldsymbol{A}^T\boldsymbol{P}\boldsymbol{A}-\boldsymbol{A}^T\boldsymbol{P}\boldsymbol{J}_0\boldsymbol{P}\boldsymbol{A} \tag{23}$$

with respect to the stabilising $\boldsymbol{P}$ and check the condition

$$\boldsymbol{R}_0 \leq \left(\boldsymbol{B}^T c\boldsymbol{P}\boldsymbol{B}+\boldsymbol{R}\right)^{-1}, \tag{24}$$

where

$$\boldsymbol{J}_0 = \boldsymbol{B}\left(\boldsymbol{I}-\boldsymbol{\Gamma}_0^2\right)\left(\left(\boldsymbol{B}^T\boldsymbol{P}\boldsymbol{B}+\boldsymbol{R}\right)\left(\boldsymbol{I}-\boldsymbol{\Gamma}_0^2\right)+\boldsymbol{R}_0^{-1}\boldsymbol{\Gamma}_0^2\right)^{-1}\boldsymbol{B}^T \tag{25}$$

(matrix $\boldsymbol{\Gamma}_0$ will be defined in due course of the paper).

3. If the inequality (22) is satisfied for $\boldsymbol{R}_0$ and $\boldsymbol{P}$, increase the elements of $\boldsymbol{R}_0$ and go to step 2; otherwise, decrease the elements of $\boldsymbol{R}_0$ and go to step 2, checking if step 4 is satisfied.

4. If the inequality (22) is satisfied for $\boldsymbol{R}_0$ and $\boldsymbol{P}$, the stabilising matrix $\boldsymbol{P}$ satisfies Equation (23), and there is no positive-definite solution for the pair $\boldsymbol{R}_0$ and $\boldsymbol{P}$ for arbitrary $\boldsymbol{R}_{0'}$, where $\boldsymbol{R}_0 \leq \boldsymbol{R}_{0'} \leq \left(\boldsymbol{B}^T\boldsymbol{P}^*\boldsymbol{P}+\boldsymbol{R}\right)^{-1}$, then stop the algorithm; in this case, the state-feedback matrix is given as:

$$\boldsymbol{F} = -\boldsymbol{\Gamma}^{-1}\left(\boldsymbol{I}-\left(\boldsymbol{X}^{-1}-\boldsymbol{R}_0\right)\left(\left(\boldsymbol{I}-\boldsymbol{\Gamma}_0^2\right)+\boldsymbol{\Gamma}_0^2\boldsymbol{R}_0^{-1}\boldsymbol{X}^{-1}\right)^{-1}\boldsymbol{\Gamma}_0^2\boldsymbol{R}_0^{-1}\right)\boldsymbol{X}^{-1}\boldsymbol{B}^T\boldsymbol{P}\boldsymbol{A}, \tag{26}$$

where $\boldsymbol{X} = \boldsymbol{B}^T\boldsymbol{P}\boldsymbol{B}+\boldsymbol{R}$.

When the following notation is introduced:

$$\boldsymbol{\Gamma} = \mathrm{diag}\{\gamma_1, \gamma_2, \ldots, \gamma_m\}, \tag{27}$$

$$\boldsymbol{\Gamma}_0 = \mathrm{diag}\{\gamma_{0,1}, \gamma_{0,2}, \ldots, \gamma_{0,m}\}, \tag{28}$$

with:

$$\gamma_i = \frac{\rho_{+,i}+\rho_{-,i}}{2}, \tag{29}$$

$$\gamma_{0,i} = \frac{\rho_{+,i}-\rho_{-,i}}{\rho_{+,i}+\rho_{-,i}}, \tag{30}$$

then the matrix $\boldsymbol{P}$ satisfying the equation:

$$\boldsymbol{P} = \boldsymbol{Q}+\boldsymbol{A}^T\boldsymbol{P}\boldsymbol{A}-\boldsymbol{A}^T\boldsymbol{P}\boldsymbol{B}\left(\boldsymbol{B}^T\boldsymbol{P}\boldsymbol{B}+\boldsymbol{R}\right)^{-1}\boldsymbol{B}^T\boldsymbol{P}\boldsymbol{A} \tag{31}$$

(the stabilising Riccatti solution to the Ricatti equation) can be presented ensuring that all eigenvalues of the matrix $\boldsymbol{A}-\boldsymbol{B}\left(\boldsymbol{B}^T\boldsymbol{P}\boldsymbol{B}+\boldsymbol{R}\right)^{-1}\boldsymbol{B}^T\boldsymbol{P}\boldsymbol{A}$ are inside the unit circle.

In addition, on the basis of (14), (27) and (28) [12]:

$$\rho = (\boldsymbol{I}+\boldsymbol{\rho}_0)\boldsymbol{\Gamma}, \tag{32}$$

$$|\boldsymbol{\rho}_0| \leq \boldsymbol{\Gamma}_0 \leq \boldsymbol{I}, \tag{33}$$

where matirx $\boldsymbol{\rho}_0 = \mathrm{diag}\{\rho_{0,1}, \rho_{0,2}, \ldots, \rho_{0,m}\}$, $\rho_{0,i} = \dfrac{\rho_i-\gamma_i}{\gamma_i}$ $(i = 1, \ldots, m)$, and operation of the absolute value $|\boldsymbol{\rho}_0|$ is elementwise for the whole matrix.

6. Actuator failure and control subject to constraints

6.1. Actuator failure and control subject to constraints

Amplitude-constrained control, where the input signals of the actuator can saturate, may be treated as a special case of actuator failure, thus one can model possible saturation of the control signals as a case of actuator failure. In such a situation, it is assumed that $\gamma_i = \alpha_i$ for $i = 1, 2, \ldots, m$, and i-th component of the constrained control vector becomes [4]

$$u^F_{i,t} = \mathrm{sat}\left(\boldsymbol{f}_i^T \boldsymbol{x}_t; \alpha_i\right), \tag{34}$$

where sat is the function that imposes constraints on the i-th component of the control vector in the span of $\pm\alpha_i$, and $\boldsymbol{f}_i^T$ is the i-th row of $\boldsymbol{F}$. The assumed failure model can also be presented for the whole control vector with $(i = 1, 2, \ldots, m)$, $u^F_{i,t} = \mathrm{sat}(\rho_i v_{t,i}; \alpha_i)$, and can be easily extended to amplitude and rate constraints either.

6.2. Simultaneous amplitude and rate constraints

Let the domain D_α of all admissible amplitude-constrained control vectors for $m = 2$ be given, as well as the domain $D_{\beta,t}$ of all admissible rate-constrained control vectors, and, as an example: $\boldsymbol{u}_{t-1} = [2.2]^T$, $\boldsymbol{v}_t = [3.2]^T$, $\alpha_1 = \pm 2$, $\alpha_2 = \pm 3$, $\beta_1 = \pm 1.3$, $\beta_2 = \pm 1.3$. Furthermore, let certain uncertainty area be given (depicted as dashed in Figs. 2c, d, 3c, d) for arbitrary $\boldsymbol{\Gamma}$ and $\boldsymbol{\Gamma}_0$. It is assumed that the set $\mathsf{D}_\alpha \cap \mathsf{D}_{\beta,t}$ is nonempty.

The method of deriving the constrained control vector is given in Fig. 2 in the situation, when directional change is allowed. When constraints (either amplitude or rate) become active, the control quality must degrade because of the windup phenomenon. The computed control vector $\boldsymbol{v}_t$ from Fig. 2a violates the amplitude constraint, thus according to the proposed method of applying constraints, its components are independently cut-off, leading to the constrained control vector as in Fig. 2b.

For the chosen levels of constraints, the cut-off action of the components of the computed control vector from (15) is depicted in Fig. 2c for $v_{1,t}$ and in Fig. 2d for $v_{2,t}$. As it can be observed, the proportions in between its components are not always kept constant, which leads to the directional change of the constrained control vector.

The dashed line resulting from the possible actuator failure, and the domain of admissible constrained control vectors resulting from rate constraints only are depicted in Figs. 2c and d. The points corresponding to the computed control vectors are also given in both the Figures. As it can be observed, they belong to the common part of sets $\mathsf{D}_{\beta_1,t}$ and $\mathsf{D}_{\beta_2,t}$ for $v_{1,t}$ and $v_{2,t}$, respectively. By taking such a constraints model into account such a situation corresponds to the the one from Section 5.

From the analysis of Figs. 2c, d we can see that the algorithm taking robustness issues into consideration comprises the case of cut-off saturation of amplitude or rate as long as for $i = 1, 2, \ldots, m$ the points $(v_{i,t}, \alpha_i \mathrm{sign}(v_{i,t}))$ lie inside m cones defining failure areas.

As an example, let us assume that $v_{1,t} \geq 0$, $\alpha_1 > 0$, and the following holds:

$$\frac{\alpha_1}{\rho_+} \leq v_{1,t} \leq \frac{\alpha_1}{\rho_-},$$

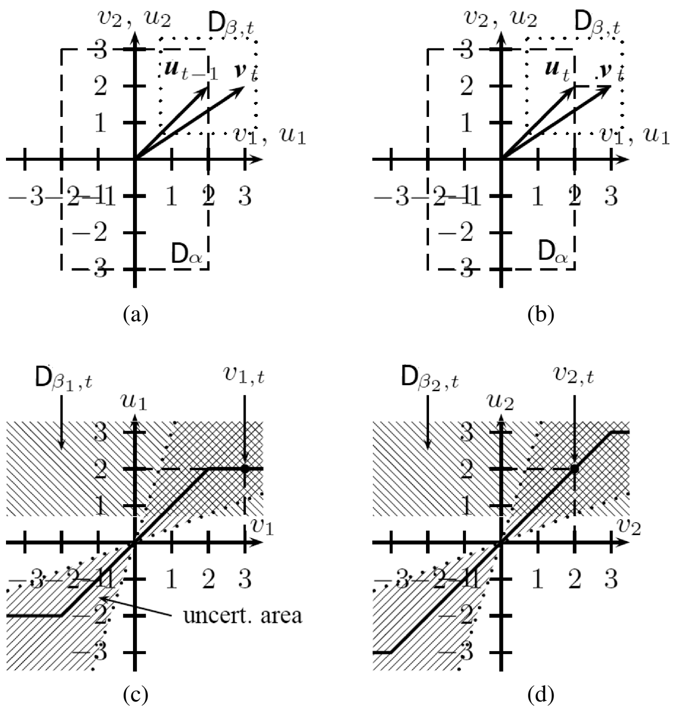

Fig. 2. Directional-changing constraint as an actuator failure for $m = 2$ control vector components: (a) unconstrained control vector; (b) constrained control vector; (c) $v_{1,t}$ component in the uncertainty area; (d) $u_{2,t}$ component in the uncertainty area

thus the point drawn in $(v_{1,t}, u_{1,t})$ plane has ordinate between extremal values resulting from intersection of the line $u_{1,t} = \alpha_1$ with $u_{1,t} = \rho_- v_{1,t}$ and $u_{1,t} = \rho_+ v_{1,t}$. A similar relation holds in the case of the remaining $m-1$ control vector components. When the computed control vector is not in the area defining possible actuator failure, one can relax constraints, in order to apply the presented algorithm (e.g. by changing selected hard constraints into soft constraints [9] and perform the selection of the best constrained control vector).

To summarise, the amplitude constraint corresponds to the unbounded vertical strip, as in Figs. 2c, d with invariant width for a time-invariant constraints. The rate constraint corresponds to the unbounded horizontal strip with time-varying location, with respect to the previous sample of the constrained control vector. If the lower and upper boundary of $u_{i,t}$ admissible with respect to this area belong, respectively, no higher than α_i and no lower than $-\alpha_i$, then the set of all admissible constrained control vectors is nonempty.

Fig. 3 presents the analogous idea of computing the constrained control vector in the case when DP requirement must hold. In order to take both constraints into account, and avoid directional change in $\boldsymbol{v}_t$, as in Fig. 3b, one has to implement the DP algorithm from [3], which is related to the modification of at least one static characteristic to keep the direction unchanged.

In the current case, the characteristics of $u_2 - v_2$ has been modified, what has been depicted in Fig. 3d, and constrained control vector is shown in Fig. 3b. As it can be observed, the DP re-

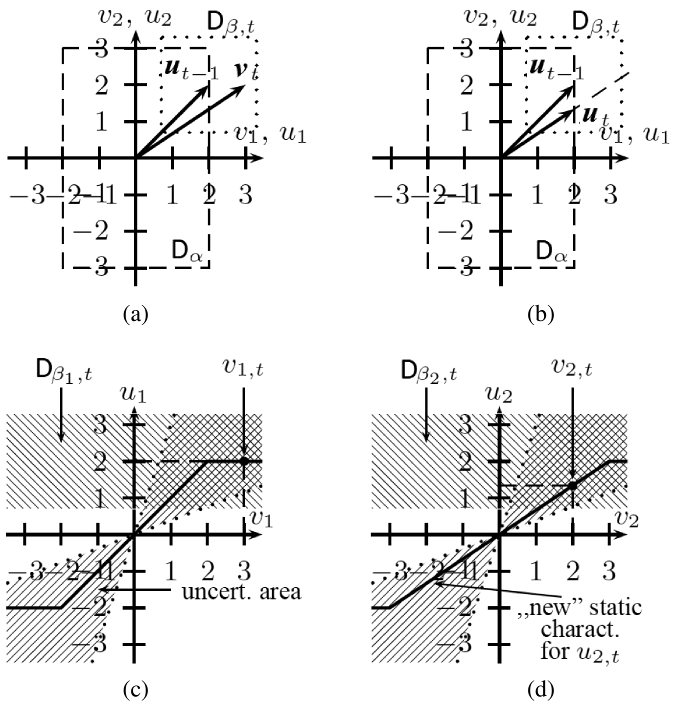

Fig. 3. Directional-preserving constraint as an actuator failure for $m = 2$ control vector components: (a) unconstrained control vector; (b) constrained control vector; (c) $v_{1,t}$ component in the uncertainty area; (d) $u_{2,t}$ component in the uncertainty area

quirement (an additional, virtual coupling between control vector components), caused the second static characteristics to approach the boundary of the area “covered” by the actuator-failure robustness algorithm. Application of this algorithm is limited to the case of minor directional change occurences, which should not be treated as an excessive limitation, because major directional changes take place only with step-like changes of, e.g. a reference vector. In the presented case, this would take place only when the computed control vector is directed mainly to one of the versors in the m-dimensional space of control vectors.

7. Simulation results

7.1. Plant model parameters

Three one-step delay controllable models are taken into consideration:

P1 $(m = 2, p = 2)$

$$\boldsymbol{A} = \begin{bmatrix} -0.80 & 0.10 & \boldsymbol{I} \\ -0.40 & 1.00 & \\ 0.49 & 0.10 & \\ -0.10 & -0.25 & \boldsymbol{0} \end{bmatrix}, \qquad \boldsymbol{B} = \begin{bmatrix} 1.0 & 0.3 \\ 0.5 & 0.8 \\ 0.0 & 0.0 \\ 0.0 & 0.0 \end{bmatrix},$$

P2 $(m = 3,\ p = 2)$

$$A = \begin{bmatrix} -0.80 & 0.10 & \multirow{2}{*}{$\boldsymbol{I}$} \\ -0.40 & 1.00 & \\ 0.49 & 0.10 & \multirow{2}{*}{$\boldsymbol{0}$} \\ -0.10 & -0.25 & \end{bmatrix}, \qquad B = \begin{bmatrix} 1.0 & 0.2 & 0.3 \\ 0.5 & 0.3 & 0.8 \\ 0.0 & 0.0 & 0.0 \\ 0.0 & 0.0 & 0.0 \end{bmatrix},$$

P3 $(m = 2,\ p = 3)$

$$A = \begin{bmatrix} 0.7 & 0.0 & -0.1 & \\ 0.1 & 0.8 & -0.2 & \boldsymbol{I} \\ -0.1 & 0.0 & 0.8 & \\ 0.1 & 0.0 & 0.0 & \\ 0.0 & -0.1 & 0.0 & \boldsymbol{0} \\ 0.0 & 0.0 & -0.5 & \end{bmatrix}, \qquad B = \begin{bmatrix} 1.0 & 0.1 \\ 0.2 & 1.0 \\ 0.5 & -0.1 \\ 0.0 & 0.0 \\ 0.0 & 0.0 \\ 0.0 & 0.0 \end{bmatrix}.$$

7.2. Performance indices

In order to verify the behavior of the control system, two performance indexes have been introduced, related to mean absolute and squared tracking errors:

$$J_1 = \frac{1}{N} \sum_{t=0}^{N} \sum_{k=1}^{p} |r_{k,t} - y_{k,t}|, \tag{35}$$

$$J_2 = \frac{1}{N} \sum_{t=0}^{N} \sum_{k=1}^{p} \left(r_{k,t} - y_{k,t}\right)^2, \tag{36}$$

where N denotes the simulation horizon.

In order to evaluate the directional change impact on the control performance, the following indices have been introduced:

$$J_{\varphi} = \frac{1}{N} \sum_{t=0}^{N} |\varphi(\boldsymbol{v}_t) - \varphi(\boldsymbol{u}_t)| \ \ [^\circ], \tag{37}$$

$$J_{\varphi^2} = \frac{1}{N} \sum_{t=0}^{N} \left(\varphi(\boldsymbol{v}_t) - \varphi(\boldsymbol{u}_t)\right)^2, \tag{38}$$

where $\varphi(\boldsymbol{v}_t)$ is an angle between the versor $\boldsymbol{e}_1$ and $\boldsymbol{v}_t$, and $\varphi(\boldsymbol{u}_t)$ is an angle between $\boldsymbol{e}_1$ and $\boldsymbol{u}_t$.

Index J_{φ} is related to mean absolute directional change (in degrees), and its value increases in proportion to the excess of the directional change. Performance index J_{φ^2} increases rapidly with severe directional change, and allows one to check what is the character of these changes.

7.3. Simulation results

The tested control system is to assure tracking of the reference vector $\boldsymbol{r}_t \in \mathrm{R}^p$, and the results have been presented in Figs. 4–8 and Tables 1–3.

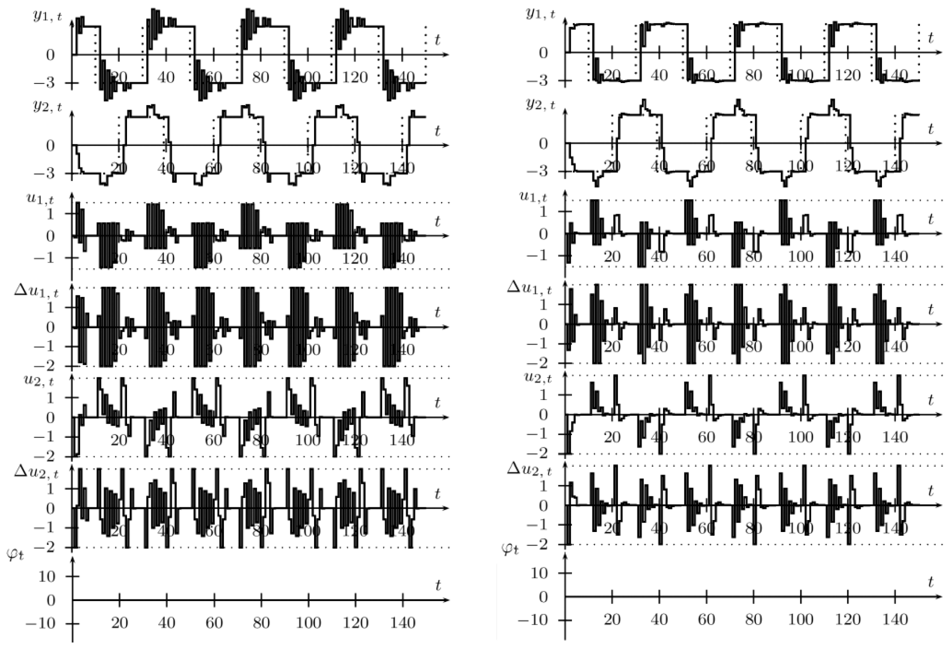

(a) (b)

Fig. 4. P1, DP control law: (a) without modeled actuator failure; (b) with robustness against actuator failure

The simulations have been carried out for the following constraints imposed on the control vector:

P1: $\alpha_1 = 1.5$, $\alpha_2 = 2.0$, $\beta_1 = 2.0$, $\beta_2 = 2.0$,

P2: $\alpha_1 = 1.5$, $\alpha_2 = 0.5$, $\alpha_3 = 1.0$, $\beta_1 = 3.0$, $\beta_2 = 0.5$, $\beta_3 = 2.0$,

P3: $\alpha_1 = 1.5$, $\alpha_2 = 2.0$, $\beta_1 = 2.0$, $\beta_2 = 2.0$,

allowing asymptotic closed-loop tracking properties, except for the case when closed-loop system becomes unstable.

Table 1. Performance indices for P1

	DP	DP + rob.	no DP	no DP + rob.
J_1	2.14	1.75	2.30	1.69
J_2	8.62	7.94	8.90	7.83
J_φ	0.00	0.00	11.30	2.74
J_{φ^2}	0.00	0.00	393.46	68.26
J	24.06	21.20	23.59	20.98

On the basis of the results presented in Tables 1–3 one can see, that introduction of DP requirement leads to increase in the performance indexes depicting control quality. Nevertheless,

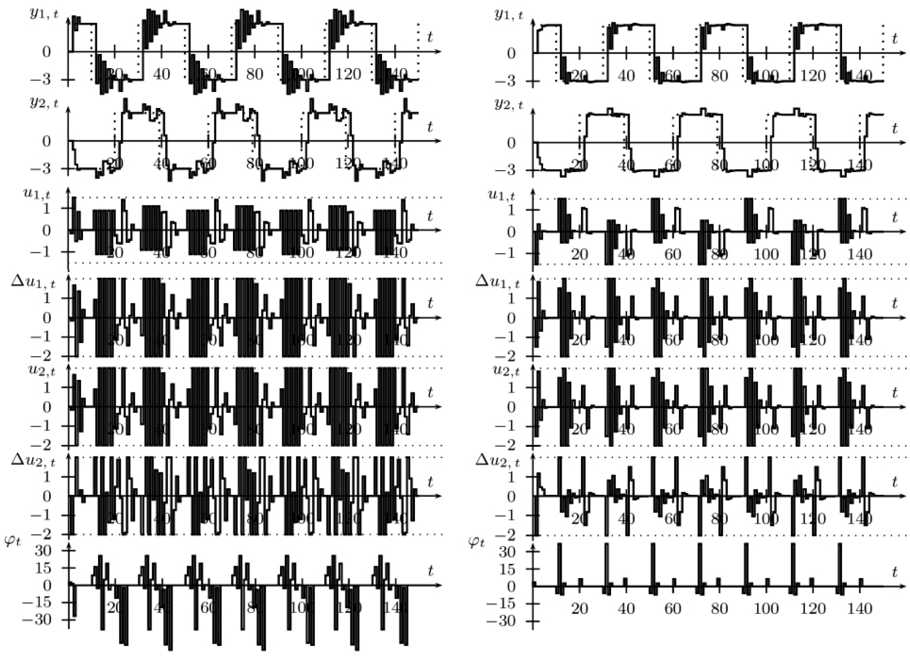

(a) (b)

Fig. 5. P1, control law with no DP: (a) without modeled actuator failure; (b) with robustness against actuator failure

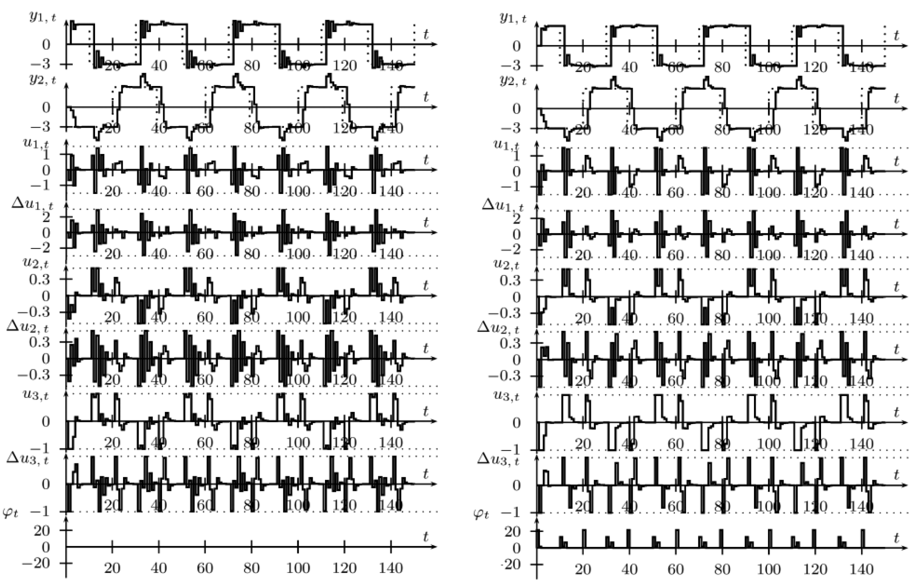

(a) (b)

Fig. 6. P2, control law with robustness against actuator failure: (a) with DP; (b) without DP algorithm

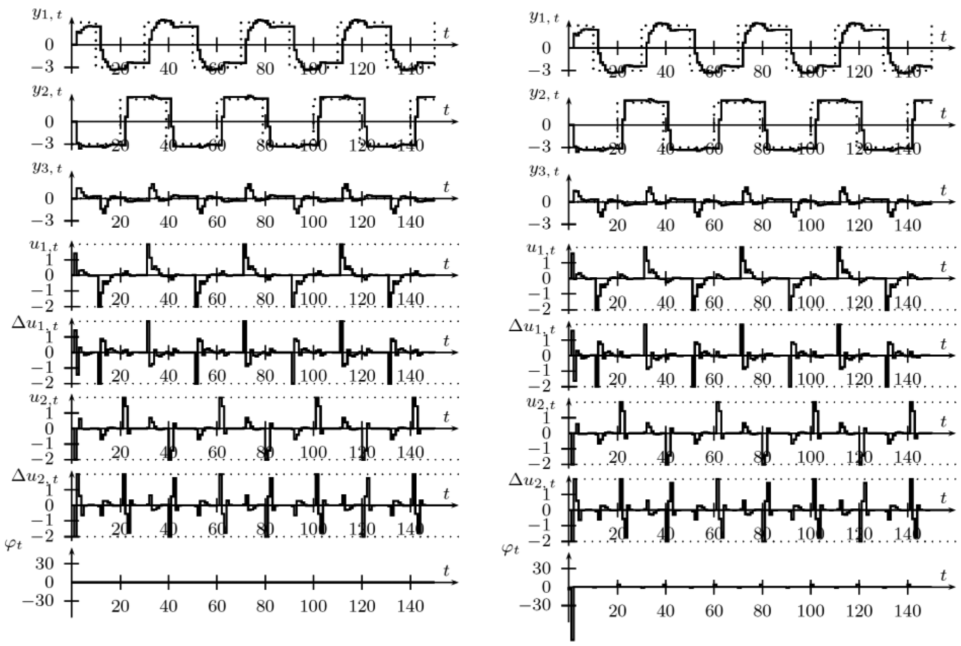

(a) (b)

Fig. 7. P3, control law without robustness against actuator failure: (a) with DP; (b) without DP algorithm

Table 2. Performance indices for P2

	DP	DP + rob.	no DP	no DP + rob.
J_1	–	4.42	–	1.69
J_2	–	11.18	–	7.83
J_φ	–	0.00	–	2.74
J_{φ^2}	–	0.00	–	68.26
J	–	27.11	–	20.98

in comparison to dynamical controllers, unable to desaturate the control vector in a single step because of dynamics of the controller, it is possible to perform the desaturation in a single step.

For plants P1 and P3, introducing the robustness against actuator failure in the case when directional change is allowed, causes all the performance indexes to decrease in comparison to the case of a standard controller with and without DP requirement. What is interesting, the introduction of the robustness against actuator failure for P1 with a DP-controller, enables one to improve performance indexes, and the introduction of robustness against actuator failure to a non-DP controller causes reduction of the mean directional change in comparison to the case without the DP algorithm and without modeled uncertainty. It can also be readily seen that the

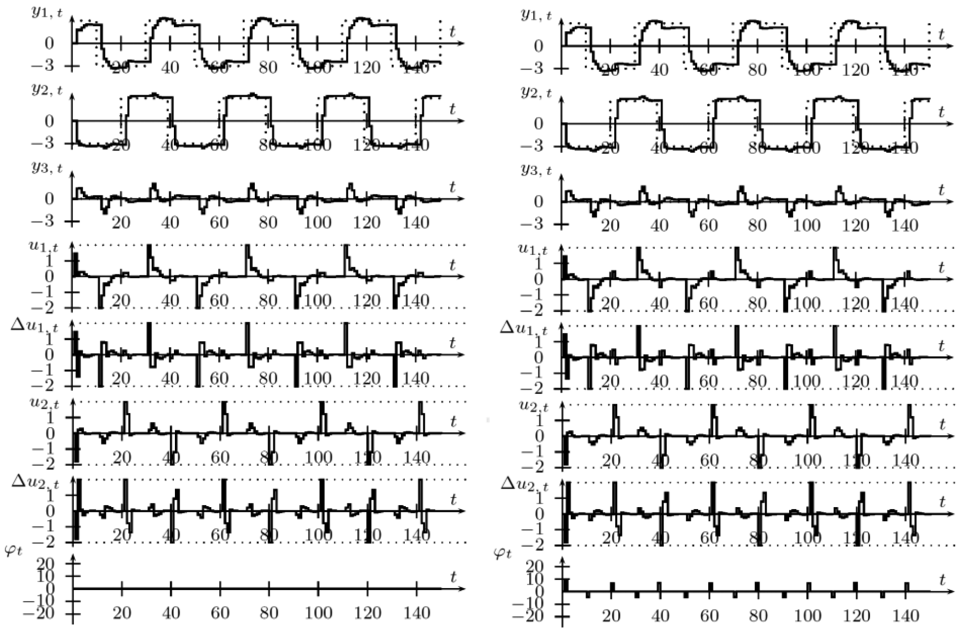

(a) (b)

Fig. 8. P3, control law with robustness against actuator failure: (a) with DP; (b) without DP algorithm

Table 3. Performance indices for P3

	DP	DP + rob.	no DP	no DP + rob.
J_1	2.47	2.48	2.48	2.50
J_2	7.86	7.86	7.86	7.87
J_φ	0.00	0.00	0.81	0.58
J_{φ^2}	0.00	0.00	49.22	3.55
J	19.21	18.92	18.90	18.86

control performance improvement does not have to be accompanied by excessive directional change (third and fourth column of Table 1).

In the case of P3, because of tight cross-coupling, as well as because $m < p$ holds, a major reduction in angular change, i.e. keeping control direction constant, leads us only to a 1% increase in performance indexes (J_1 and J_2). In such a case, the use of the DP algorithm does not cause severe performance degradation.

In the case of P2 (unstable plant), lack of robustness introduced to the control system, with imposed constraints, caused the control system to become unstable. When $m > p$ holds, a simple static controller is usually unable to stabilise the closed-loop system. Introduction of robustness causes the closed-loop system to stabilise. On the basis of plots from the tracking system, one can see that robustness against actuator failure causes less frequent resaturation of the elements of thr control vector and its rates of changes.

8. Conjectures and conclusions

The improvement in quality of control must not always, as has been here presented, be connected with increase in directional change. By introducing the robustness against actuator failure to the control system, represented as cut-off or DP nonlinearity here, it is possibile to obtain further reduction of performance indices. The improvement in windup avoidance (visible by observation of evolution of control vectors in time) goes along with preserving (or avoiding excessive changes) in control vector direction.

Conjecture 1

In a controllable LQR-controlled system for $m \leq p$ taking robustness against the actuator failure into account improves the performance indices, and, in addition, in the $m = p$ case with cut-off saturation, enables further reduction of the directional change with respect to the analogous case but without the robustness algorithm.

Conjecture 2

In the case of $m < p$, having introduced DP requirement causes neglectful increase in performance indices, which creates the possibility of keeping the original control vector direction virtually with no loss in quality in comparison with the case of cut-off saturation. Taking robustness issues into account allows one to reduce the frequency of saturations of the control vectors.

References

[1] Albertos P., Sala A., *Multivariable Control Systems*, Springer (2002).

[2] Giernacki W., *Near to Optimal Design of PI$^{\lambda}$D$^{\mu}$ Fractional-Order Speed Controller (FOPID) for Multirotor Motor-rotor Simplified Model*, 17th International Conference on Unmanned Aircraft Systems, Arlington, pp. 320–326 (2016).

[3] Horla D., *On directional change and anti-windup compensation in multivariable control systems*, International Journal of Applied Mathematics and Computer Science, vol. 19, no. 2, pp. 281–289 (2009).

[4] Horla D., Królikowski A., *Discrete-time LQG Control with Actuator Failure*, 8th International Conference on Informatics in Control, Automation and Robotics, Noordwijkerhout, CD-ROM (2011).

[5] Hu T., Lin Z., *Control systems with actuator saturation: Analysis and design*, Birkhäuser, (2001).

[6] Maciejowski J.M., *Multivariable Feedback Design*, Addison-Wesley Publishing Company (1989).

[7] Maciejowski J.M., *Predictive Control with Constraints*, Pearson Education Limited (2002).

[8] Mahmoud M.S., *Resilietn Control of Unvertain Dynamical Systems*, Springer (2004).

[9] Petersen I.R., McFarlane D.C., *Optimizing the guaranteed cost in the control of uncertain systems*, in Mansour M., Balemi S., Truol W. (Eds.), *Robustness of dynamical systems with parameter uncertainties*, Brikhäuser (1992).

[10] Tarbouriech S., Gomes da Silva, J., *Synthesis of controllers for continuoustime delay systems with saturating controls via LMIs*, IEEE Transactions on Automatic Control, vol. 45, no. 1, pp. 105–111 (2000).

[11] Xie L., Soh Y.C., *Guaranteed cost control of uncertain discrete-time systems*, Control Theory and Advanced Technology, vol. 10, pp. 1235–1251 (1995).

[12] Yang Y., Yang G.-H., Soh Y.C., *Reliable Control of Discrete-time Systems with Actuator Failures*, IEE Proceedings – Control Theory and Applications, vol. 147, no. 4, pp. 428–432 (2000).

[13] Yang G.-H., Wang J.L., Soh Y.C., *Reliable LQG Control with Sensor Failures*, IEE Proceedings – Control Theory and Applications, vol. 147, no. 4, pp. 433–439 (2000).

[14] Ziętkiewicz J., *Non-minimum Phase Properties and Feedback Linearization Control of Nonlinear Chemical Reactor*, 20th International Conference on Methods and Models in Automation and Robotics, CD-ROM (2015).

[15] Zuo Z., Ho D.W.C., Wang Y., *Fault Tollerant Control for Singular Systems with Actuator Saturation and Nonlinear Perturbation, Automatica*, vol. 46, pp. 569–576 (2010).